Supporting information

Elevated temperature-driven coordinative reconstruction of unsaturated single-Ni-atom structure with low-valency on a polymer-derived matrix for electrolytic oxygen evolution reaction

Rahul Patil[a], Anubha Rajput[b], Babasaheb M. Matsagar[c], Norman C. R. Chen[c,d,e], Masaki Ujihara[f], Rahul R. Salunkhe[g], Praveen Yadav[h], Kevin C.-W. Wu[c*], Biswarup Chakraborty[b*], Saikat Dutta[a*]

[a] Electrochemical Energy & Sensor Research Laboratory, Amity Institute of Click Chemistry Research & Studies, Amity University, Noida, India

[b] Department of Chemistry, Indian Institute of Technology, New Delhi, India

[c] Department of Chemical Engineering, National Taiwan University, Taipei 10617, Taiwan

[d] Molecular Science and Technology Program, Taiwan International Graduate Program Academia Sinica, Taiwan

[e] International Graduate Program of Molecular Science and Technology (NTU-MST), National Taiwan University, Taiwan

[f] Graduate Institute of Applied Science and Technology, National Taiwan University of Science and Technology, Taipei, Taiwan

[g] Materials Research Laboratory Department of Physics, Indian Institute of Technology, Jammu, India

[h] Synchrotron X-ray Facility, Raja Ramanna Centre for Advanced Technology, Rajendra Nagar, Indore, Madhya Pradesh 452013

Experimental Section:

Reagents: Nickel acetate tetrahydrate, 2-Methyl Imidazole, cetyltrimethylammonium bromide (CTAB), were obtained from sigma Aldrich. Ethanol was purchased from shangzu, China. All chemicals are analytical grade and used without further purification.

Synthesis of ZIF-8

ZIF-8 polyhedra were prepared by the following method. Typically, 600 mg of $Zn(CH3COO)_2 \cdot 2H_2O$ was dissolved in 10 mL of water and 1.12 g of MeIM and 2.0 mg of cetyl trimethylammonium bromide (CTAB) were dissolved in 10 mL of water by sonication. Then the solution of $Zn(CH_3COO)_2$ was added to the solution of MeIM and CTAB, and gently stirred for 10 s. The mixture was left undisturbed at room temperature (RT) for 12 h. The resulting ZIF-8 were washed with deionized (DI) water and ethonal using centrifuge and dried in vaccum oven at 80 ^oC for 12 hours.

Synthesis of Ni-phen@ZIF

First, a mixture of $Ni(CH_3COO)_2 \cdot 4H_2O$ (0.5 mmol) and 1,10-phenanthroline (1.5 mmol) was added to 10 mL ethanol and stirred at 60 ^oC. Then, the as-prepared ZIF-8 (900 mg) was added to the above mixed solution and vigorous stirred until all the solvent evaporated. The product was finely ground and named as Ni-phen@ZIF-8.

Synthesis of Ni-phen@ZIF-8-RF

Resorcinol (15mg), formaldehyde solution (3g) and CTAB (15 mg) were first dissolved in 60 ml of deionized water with stirring for 30 min. Then, 200 mg of Ni-phen@ZIF-8 was dispersed and sonicated for 10 min, followed by stirring for 24 h at room temperature. The resulting precipitate was collected by centrifugation, washed and dried under a vacuum overnight. The product was named Ni-phen@ZIF-8-RF.

Synthesis of NiSA-NC-900 or Ni-N_x/NC

The as-prepared Ni-phen@ZIF-8-RF was transferred to a tube furnace, and then maintained at 900 °C for 120 min with a heating rate of 5 °C min^{-1} under Ar flow. The resulting product was cooled to room temperature and washed with 1 M H_2SO_4 extensively to remove unstable metallic species and Zn^{+2} residues. After that, the resulting material was dried at 80 °C. The final product is referred to as NiSA-NC-900. Additionally, NiNP-NC-700 was prepared with same procedure by appling the 700 °C temprature for 2 hours with with a heating rate of 5 °C min^{-1} under Ar flow.

Characterization

Co and Ni K-edge X-ray absorption data were acquired in transmission mode at room temperature on bending magnet station 12-BM-B at the Advanced Photon Source (National Synchrotron Radiation Research Center, Taiwan) with a Rh focusing mirror and Si (111) monochromator. The incident X-ray energy was calibrated using Co and Ni foil (EXAFS Materials) by setting the inflection point in the first differential XANES. The XAS data were processed and analyzed with Athena software including background removal, edge-step normalization, and Fourier transform.

Electrochemical Experiments:

Preparation and deposition of catalyst ink on the electrode surface.

Three dimensional and porous network like nickel foam (NF) of thickness ca. 0.5 mm were chosen as electrode substrates for catalyst deposition. The following steps were sequentially employed to prepare a catalyst ink and subsequently to deposit it on NF: (i) The sheet of NF was cut in several pieces of dimension 1x2 cm^2. It was then washed ultrasonically in 0.1 N HCl followed by washing twice with milli-Q water and once with acetone. The electrodes were then dried at 50^{o}C overnight in an oven. (ii) To prepare the ink, Nafion was used as a medium to disperse the catalyst in aqueous medium. Nafion is a conductive, sulfonated

tetrafluoroethylene-based fluoropolymer which binds the catalyst particles on the electrode surface.[1] Nafion was diluted to 1.0 wt% in ethanol and 50 mg NiSA-NC-900 was added into it. The mixture was homogenized by sonicating it for 10 minutes at room temperature. (iii) The prepared ink was drawn in a pipette and was deposited dropwise on pre-cleaned NF surface. The 1x1 cm^2 surface area was covered with the ink after which the electrode was left to dry at room temperature overnight. Similarly, electrodes were prepared for other reference compounds.

Electrochemical measurement. To study the electrocatalytic water splitting activity, a potentiostat (Gamry Interface 1010E) instrument controlled by Echem Analyst™ Software was used for electrochemical measurements and the Origin software was used to further analyze the data. The electrochemical study was done typically in a three-electrode system using 1 M KOH electrolyte (pH 13.6). Among the three electrodes, NF loaded with catalyst was used as a working electrode (WE), A platinum coil electrode was used as a counter electrode (CE) and a Hg/HgO electrode (E^o = 0.098 V vs. RHE) was used as a reference electrode (RE).

The CV and LSV were measured to study the electrochemical OER. The electrochemical measurement (CV and LSV) was done with a manual iR compensation (R = resistance of solution including the test electrode) of 85%, in which the value of uncompensated resistance was obtained from the impedance study. In 1 M KOH, the reference potential with respect to Hg/HgO was converted to potentials in reference to Reversible Hydrogen Electrode (RHE) by using following relation (equation 1):

$$E(RHE) = E\left(\frac{Hg}{HgO}\right) + 0.098V + (0.059 \times pH)V \qquad \text{Equation 1}$$

To study the oxygen evolution reaction (OER), the potential range 1.0 V to 1.8 V (*vs*. RHE) was used with a scan rate of 1 mV s^{-1}. The obtained polarographs were used to calculate the overpotential at a fixed current density. CV is an extended form of LSV in which potential is

swept linearly with time in a complete cycle. CV was performed for 10 cycles prior to LSV in order to activate the catalyst.

Tafel slopes are calculated from the slope of the overpotential (η) versus the logarithm of current density (log *j*) plot and the slope was determined from the kinetically controlled region of the curve. The Tafel slope was calculated according to the Tafel equation:

$$\eta = b\log j + a \qquad \text{Equation 2}$$

where η is the overpotential (V), *j* is the current density (mA cm^{-2}), a and b are the Tafel slope (mV dec^{-1}).

Out of the deposited amount of catalyst, the fraction of it taking part in the catalytic activity is determined by ECSA. The ECSA in turn is obtained from the double layer capacitance (C_{dl}) of the catalyst which was determined by recording cyclic voltammograms of each catalyst in a non-faradic region of 0.8953 V to 0.9953 V (*vs.* RHE) in 1 M KOH at varying scan rates (i.e., 10, 25, 50, 100, 150, and 200 mV s^{-1}). To determine the C_{dl}, the charging current was measured from each redox half of the CV curve at midway potential which was then plotted against scan rate to obtain a linear slope. This slope represents the C_{dl} at the electrode-electrolyte interface.[83] The ESCA was calculated from the following equation.

$$ESCA = \frac{C_{dl}}{C_s} \qquad \text{Equation 3}$$

The value of C_s indicates the specific capacitance of the material per unit area under identical electrolytic conditions. In 1M KOH solution the C_s value for NF is 0.04 mF cm^{-2}.[2]

The CA study was done to study the stability of the catalyst i.e., its durability without substantial loss in activity. CA was performed in 1 M KOH, for 12 h at a constant potential.

Electrochemical impedance spectroscopy (EIS) was recorded in a frequency region of 100 mHz to 1 MHz and the obtained data is plotted as ReZ vs Im Z (Nyquist plot). The obtained semi-circular data in the Nyquist plot was fitted into an equivalent RC circuit model. The charge-transfer resistance (R_{ct}) of the electrode was determined with the help of the semicircle of the Nyquist plot where the impedance at higher frequency region denotes the solution resistance (R_s) and the difference between impedance at higher and lower frequency represents the R_{ct}.[3]

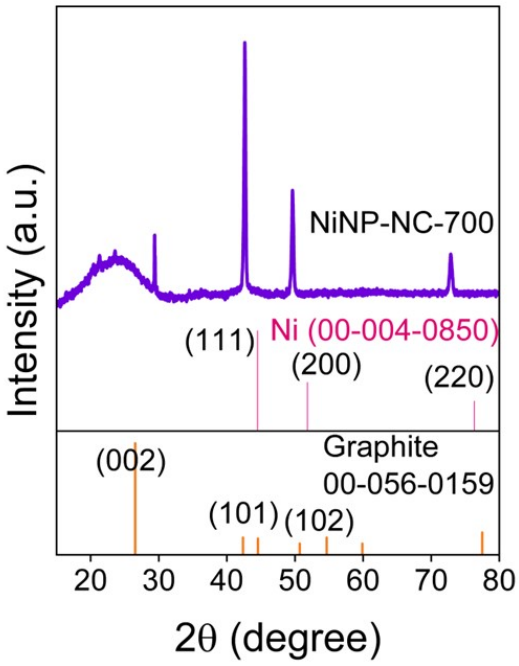

Figure S1. XRD pattern of NiNP-NC-700.

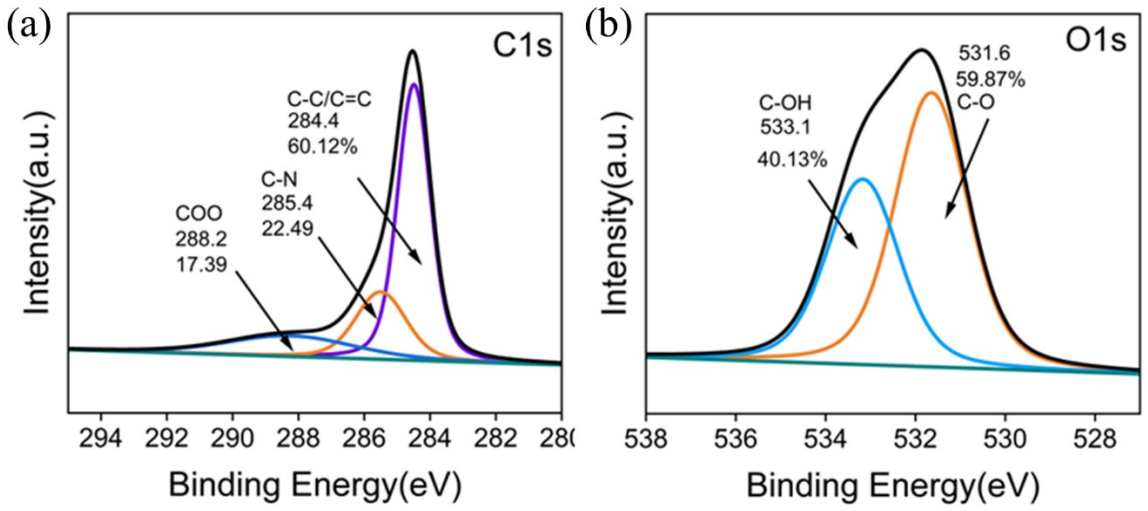

Figure S2. XPS spectral pattern of NiSA-NC-900 for (a) C1s, (b) O1s.

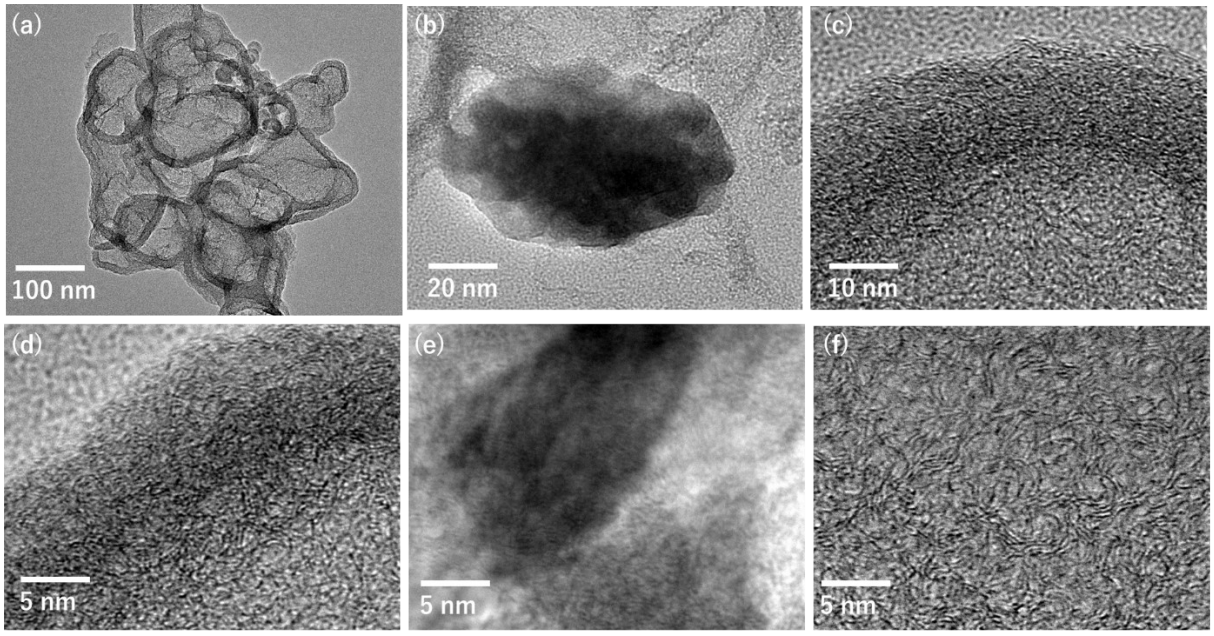

Figure S3. Section of HR-TEM at (a) 100 nm (b) 20nm (c) 10nm and (d-f) 5nm scale respectively for NiSA-NC-900.

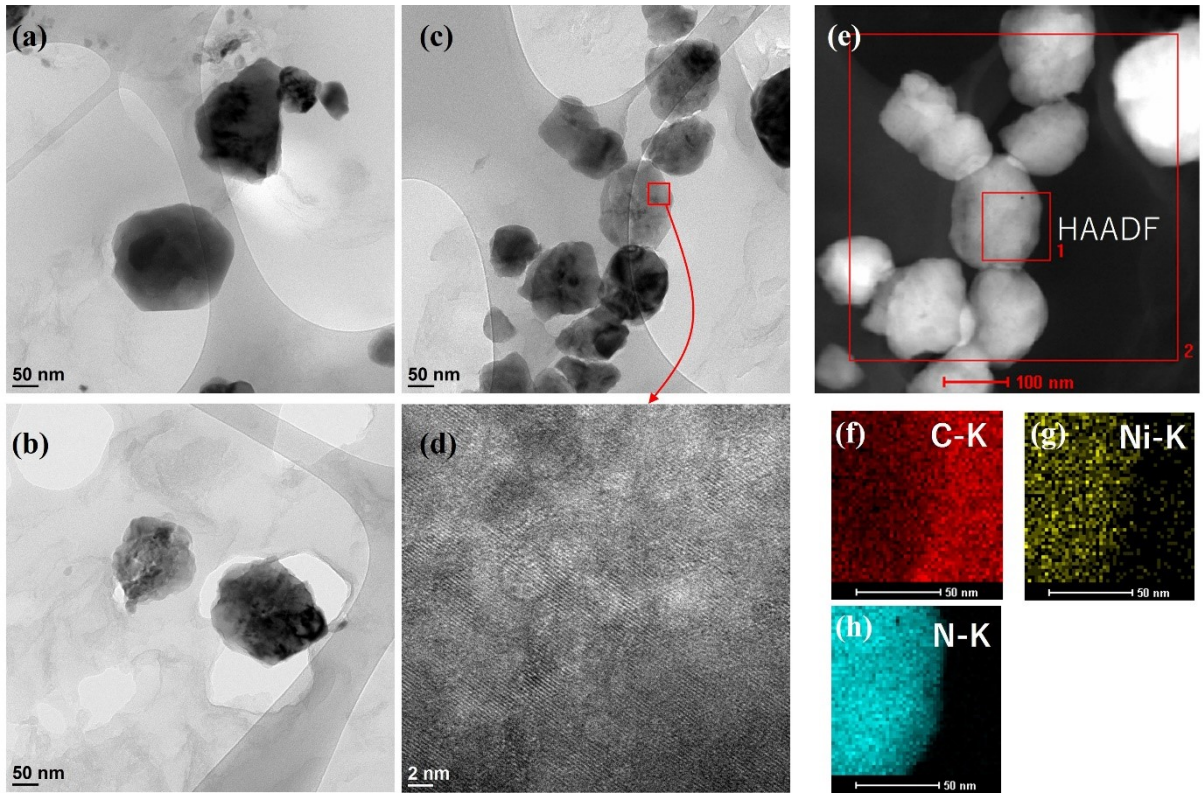

Figure S4. Section of HR-TEM at (a-c) 50 nm scale and (d) 2 nm (e-h) HAADF-STEM of Ni-NP-NC-700.

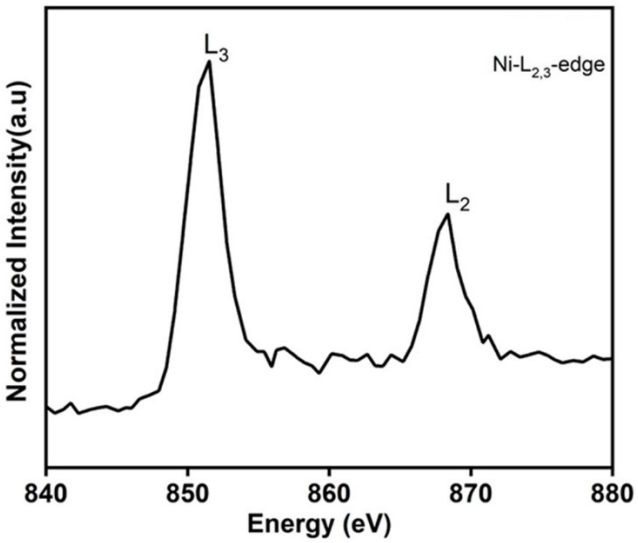

Figure S5. Soft X-ray absorption spectra of Ni-L_3-edge of NiSA-NC-900.

Table S1. Structural parameters of NiSA-NC-900 extracted from the EXAFS fitting.

Scattering pair	CN	R(Å)	$\sigma^2(10^{-3}Å^2)$	S02	ΔE_0(eV)	R factor
Ni-N	2.000	1.703	0.013	-1.490	0.457	0.008

S02 is the amplitude reduction factor; CN is the coordination number; R is interatomic distance (the bond length between central atoms and surrounding coordination atoms); σ2 is Debye-Waller factor (a measure of thermal and static disorder in absorber-scatterer distances); ΔE0 is edge-energy shift (the difference between the zero kinetic energy value of the sample and that of the theoretical model). R factor is used to value the goodness of the fitting.

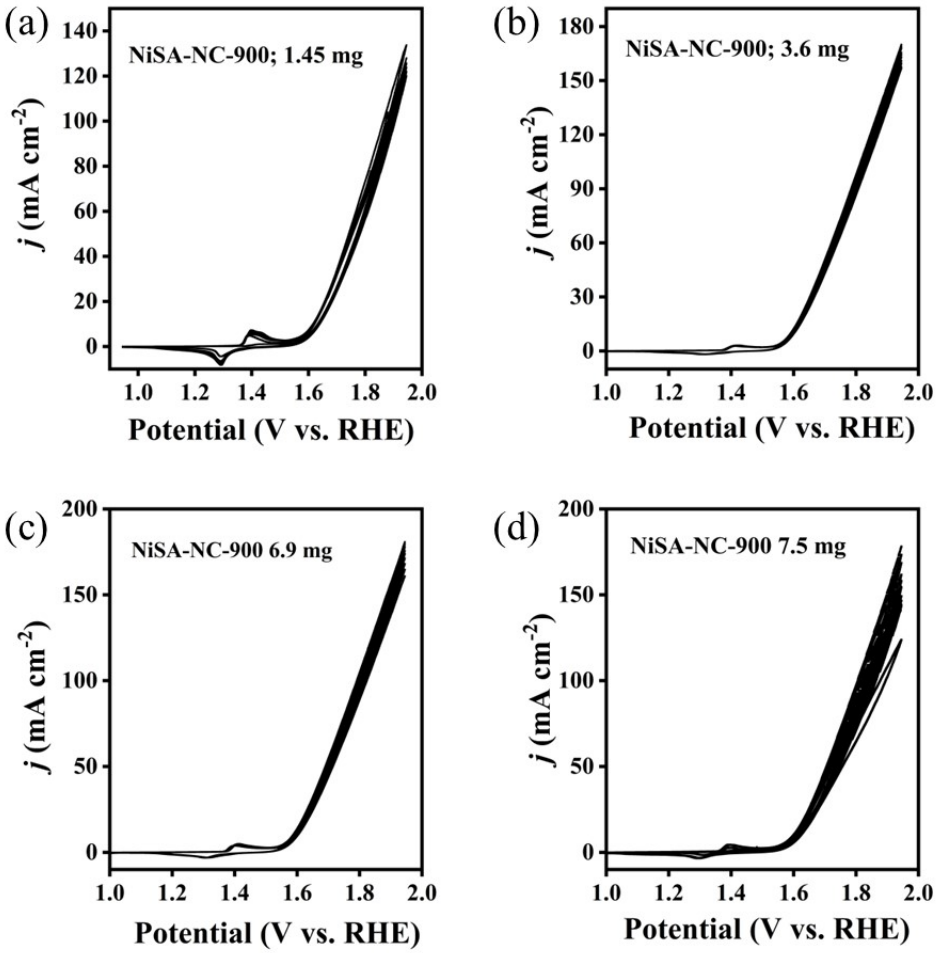

Figure S6. CV cycles recorded with differently loaded NiSA-NC-900/NF as anode at a scan rate of 5 mV s^{-1} (without iR compensation).

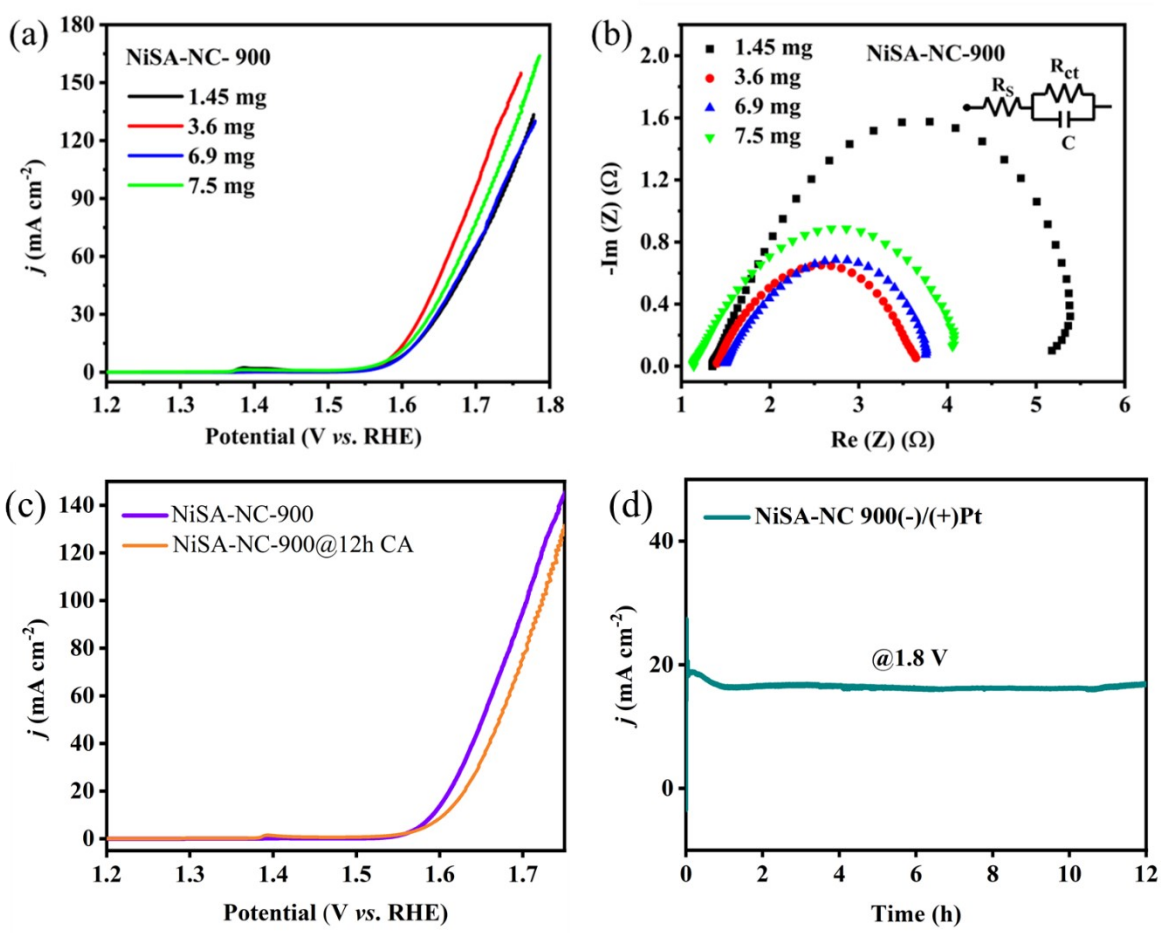

Figure S7. (a) Polarization curves obtained from the LSV recorded with different loading of Ni SA 900/NF with a scan rate of 1 mV s^{-1} (with 85% iR correction). (b) EIS study of electrodes for different loading of Ni SA 900/NF. (c) Polarization curves obtained from the OER-LSV study with NiSA-NC-900/NF before and after 12h OER-CA at a constant potential of 1.615 (V vs. RHE). (d) Chronoamperometric study with NiSA-NC-900(-)/(+)Pt electrolyzer at a cell potential of 1.8 V for 12 h.

Table S2: The overpotential recorded at a *j* value of 10 mA cm^{-2} and charge transfer resistance from the OER-LSV curves using different amounts of NiSA-NC-900/NF loaded electrodes.

Catalyst ink loading	Mass loading (mg)	η(mV)@10 mA	R_{ct} (Ω)
50	1.45	370	3.82
100	3.6	362	2.23
150	6.9	376	2.25
200	7.5	365	2.91

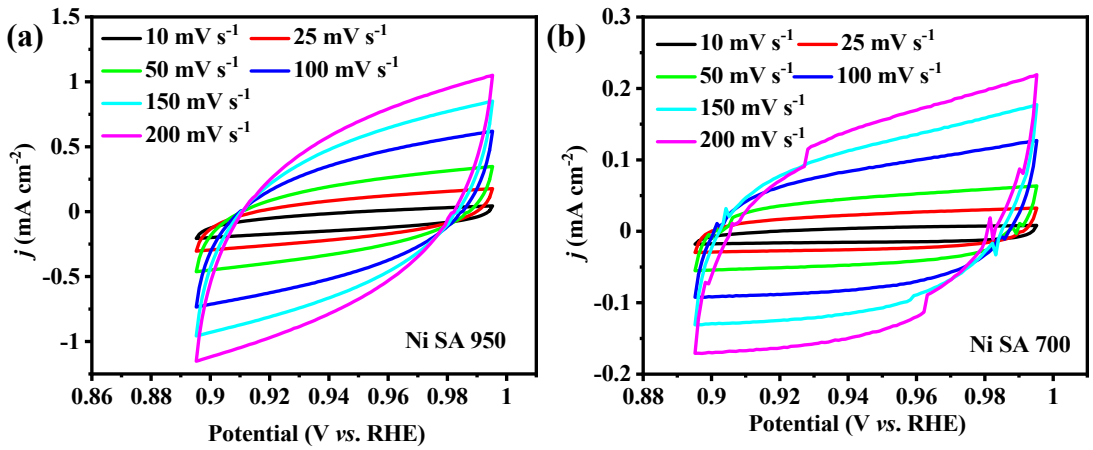

Figure S8. CV scans in a non-Faradaic potential range of (a) NiSA-900-NC/NF (b) NiNP-NC-700/NF in 1 M KOH at scan rate of 50 mV s^{-1}, 100 mV s^{-1}, 150 mV s^{-1}, 200 mV s^{-1} and 250 mV s^{-1}. Half of the differences in current density variation ($\Delta J = (J_{cathodic}-J_{anodic})/2$) at a potential of 0.94 V vs RHE plotted against scan rate fitted to a linear regression enables the determination of double-layer capacitance (C_{dl}). C_{dl} value calculated from the slopes of the linear fitting of Δj (mA cm^{-2}) *vs.* scan rate (mV s^{-1}).

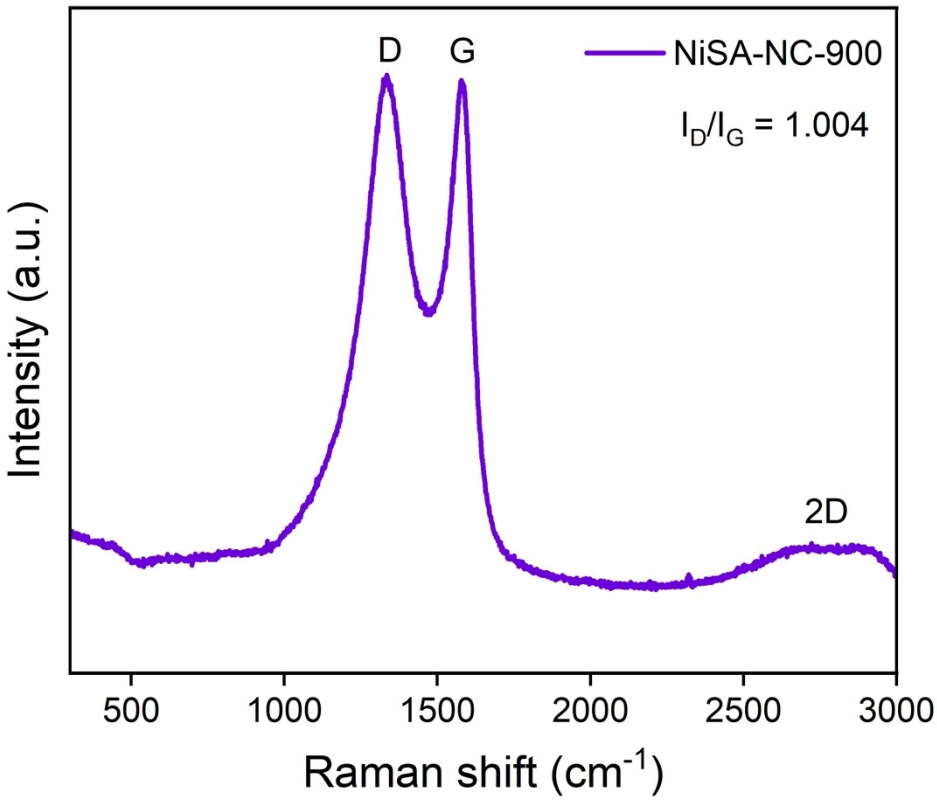

Figure S9. Raman spectra of NiSA-NC-900

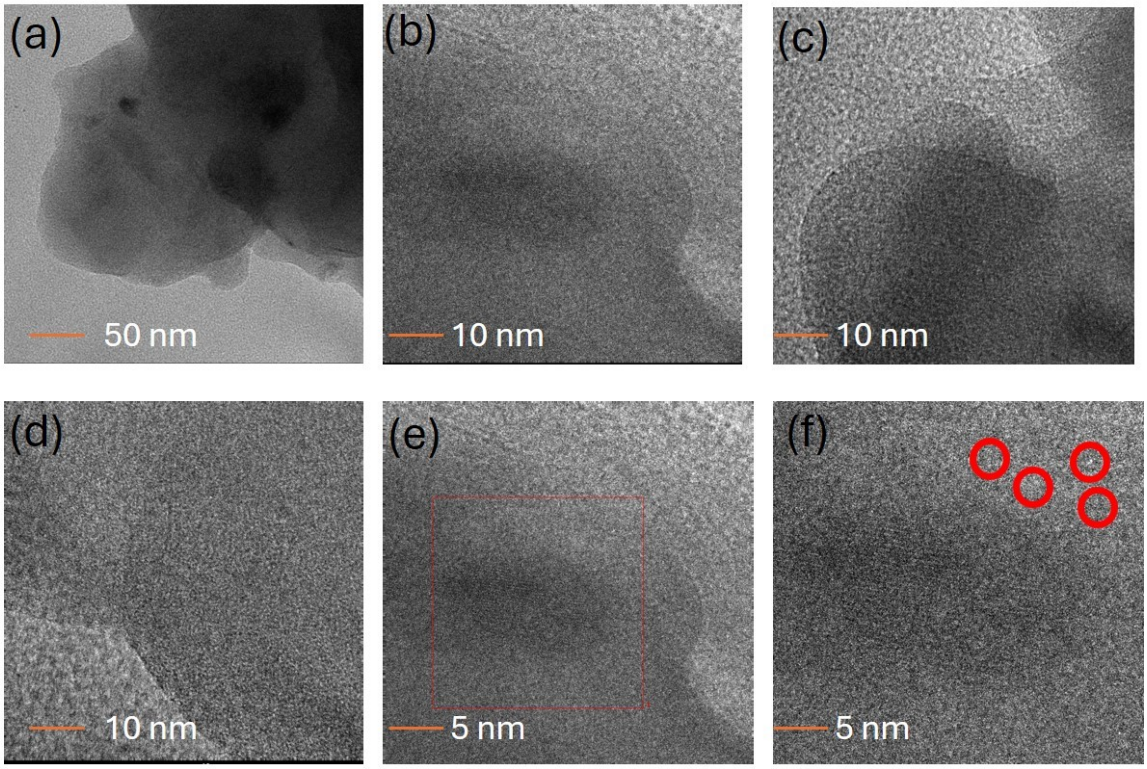

Figure S10. HR-TEM analysis of post-OER (12h) NiSA-NC-900. (a-d) TEM images with N-C structure. (e) Identification of lattice planes of N–C matrix. (f) Identification of lattice planes of N–C with atom sites.

Table S3. The comparison of the different electrochemical parameters of NiSA-NC-900/NF and NiNP-NC-700/NF.

Catalyst	Mass loading (mg)	η(mV)@10 mA	Tafel (mV)	R_{ct} (Ω)	C_{dl} (mF)
NiSA-NC-900	3.6	362	39.68	2.237	3.19
NiNP-NC-700	3.3	375	56.9	3.48	0.7

Table S4. The comparison of the OER activity parameters of NiSA-NC-900/NF with similar single-Ni-atom systems consisting with Ni–N_x or Ni–O atomic sites.

Entry	Single-atom electrode	Electrolyte (M KOH)	OP at 10 mA cm^{-2} [mV]	TS [mV dec^{-1}]	Stability at room temperature	Refs.
1	Ni-NHGF	1	331	63	20 h at 10 mA cm^{-2}	[4]
2	Ni-O-G SACs	1	224	42	50 h at OP of 400 mV	[5]
3	Ni-O-G SACs	1	328	84	50 h at 10 mV cm^{-2}	[6]
4	NiN_3	1	250	45	Retained 92%% of performance after 18h at OP 0.4V	[7]
5	Ni_3C/C	1	240	46	~14h at OP of 0.32V	[8]
6	Ni_xB	1	380	89	60 h at 10 mA cm^{-2}	[9]
7	NiSAs@S/N-CMF	1	285	50.8	-	[10]
8	NiSA-NC-900	1	362	39.68	12 h at ~16 mA cm^{-2} in OWS	This work

References

1. N. Yusoff, in *Graphene-Based Electrochemical Sensors for Biomolecules*, eds. A. Pandikumar and P. Rameshkumar, Elsevier, 2019, DOI: https://doi.org/10.1016/B978-0-12-815394-9.00007-8, pp. 155-186.
2. C. C. L. McCrory, S. Jung, J. C. Peters and T. F. Jaramillo, *Journal of the American Chemical Society*, 2013, **135**, 16977-16987.
3. R. Beltrán-Suito, P. W. Menezes and M. Driess, *Journal of Materials Chemistry A*, 2019, **7**, 15749-15756.
4. H. Fei, J. Dong, Y. Feng, C. S. Allen, C. Wan, B. Volosskiy, M. Li, Z. Zhao, Y. Wang, H. Sun, P. An, W. Chen, Z. Guo, C. Lee, D. Chen, I. Shakir, M. Liu, T. Hu, Y. Li, A. I. Kirkland, X. Duan and Y. Huang, *Nature Catalysis*, 2018, **1**, 63-72.
5. Y. Li, Z.-S. Wu, P. Lu, X. Wang, W. Liu, Z. Liu, J. Ma, W. Ren, Z. Jiang and X. Bao, *Adv. Sci.*, 2020, **7**, 1903089.
6. F. Wang, H. Zhao, Y. Ma, Y. Yang, B. Li, Y. Cui, Z. Guo and L. Wang, *Journal of Energy Chemistry*, 2020, **50**, 52-62.
7. K. Xu, P. Chen, X. Li, Y. Tong, H. Ding, X. Wu, W. Chu, Z. Peng, C. Wu and Y. Xie, *J. Am. Chem. Soc.*, 2015, **137**, 4119-4125.
8. K. Xu, H. Ding, H. Lv, P. Chen, X. Lu, H. Cheng, T. Zhou, S. Liu, X. Wu, C. Wu and Y. Xie, *Adv. Mater.*, 2016, **28**, 3326-3332.
9. J. Masa, I. Sinev, H. Mistry, E. Ventosa, M. de la Mata, J. Arbiol, M. Muhler, B. Roldan Cuenya and W. Schuhmann, *Adv. Energy Mater.*, 2017, **7**, 1700381.
10. Y. Zhao, Y. Guo, X. F. Lu, D. Luan, X. Gu and X. W. Lou, *Adv. Mater.*, 2022, **34**, 2203442.